

Fluctuations in the number of particles adsorbed under the influence of diffusion and flow

Zbigniew Adamczyk, Barbara Siwek, Lilianna Szyk, and Maria Zembala

Citation: *The Journal of Chemical Physics* **105**, 5552 (1996); doi: 10.1063/1.472396

View online: <http://dx.doi.org/10.1063/1.472396>

View Table of Contents: <http://scitation.aip.org/content/aip/journal/jcp/105/13?ver=pdfcov>

Published by the [AIP Publishing](#)

Articles you may be interested in

[Kinetics of the \$A+B\rightarrow 0\$ reaction under steady and turbulent flows](#)

J. Chem. Phys. **105**, 10925 (1996); 10.1063/1.472896

[Molecular dynamics study of tracer diffusion of argon adsorbed on amorphous surfaces](#)

J. Chem. Phys. **105**, 9674 (1996); 10.1063/1.472797

[Tracer diffusion of highly charged polymer colloids](#)

J. Chem. Phys. **105**, 9625 (1996); 10.1063/1.472793

[Fluctuationdominated \$A+B\rightarrow 0\$ kinetics under shortranged interparticle interactions](#)

J. Chem. Phys. **105**, 6304 (1996); 10.1063/1.472466

[Random sequential adsorption of spheroidal particles: Kinetics and jamming limit](#)

J. Chem. Phys. **105**, 5562 (1996); 10.1063/1.472409



Fluctuations in the number of particles adsorbed under the influence of diffusion and flow

Zbigniew Adamczyk,^{a)} Barbara Siwek, Lilianna Szyk, and Maria Zembala
*Institute of Catalysis and Surface Chemistry, Polish Academy of Sciences, 30-239 Cracow,
Niezapominajek 1, Poland*

(Received 25 March 1996; accepted 20 June 1996)

Fluctuations in the number of colloid particles adsorbed irreversibly under diffusion and flow were determined. The experimental measurements were carried out in the impinging-jet cells using as model colloids the monodisperse polystyrene latex particles of micrometer size range adsorbing at mica sheets. The surface concentration of adsorbed particles was determined quantitatively using the direct microscope observation method coupled with an image analyzing system. Two series of experiments were performed (i) for diffusion controlled adsorption when the random sequential adsorption (RSA) mechanism was valid and (ii) for flow controlled adsorption. It was found that in the case of RSA the reduced variance of the distributions decreased markedly for increasing surface concentration θ in accordance with theoretical predictions based on the mean-field approximation. The experimental results were in a good agreement with the numerical simulations performed according to the RSA algorithm. It was also determined that the magnitude of fluctuations in our irreversible system was very similar to reversible systems described by the scaled-particle theory. A significantly different behavior was observed for flow affected adsorption when the reduced variance (at the same surface concentration) was much smaller than for the RSA model, therefore deviating considerably from an equilibrium system. The decrease in the variance indicated that the surface exclusion effects (described by the available surface function) were more important under flow due to the hydrodynamic scattering effect. © 1996 American Institute of Physics. [S0021-9606(96)50936-0]

I. INTRODUCTION

Interactions of macromolecules, colloid, and bioparticles (proteins, enzymes, viruses, bacteria, etc.) with solid/liquid interface leading to adsorption and adhesion are of practical significance for polymer and colloid science, biophysics, and medicine, enabling a better understanding and control of protein and cell separation processes, enzyme immobilization, biofouling of transplants and artificial organs, etc.

Since adsorption of these particles is often irreversible¹⁻³ the surface concentration of particles does not uniquely define the properties of a given system. Thus, it was deduced theoretically⁴⁻⁷ and confirmed experimentally^{3,8-10} that the available surface function (ASF) ϕ for the same surface concentration θ can be different, depending on the detailed topology of particle distributions. The distributions are influenced in turn by the adsorption mechanism of particles, either diffusion,³ sedimentation,^{8,9,11-14} or flow¹⁰ whose relative significance can be characterized by the two dimensionless parameters³

$$Ex = V_m a / D_\infty,$$

$$Pe = V_h a / D_\infty,$$

where Ex is the external force parameter, V_m is the charac-

teristic migration velocity of a particle under external force (e.g., gravity or magnetic force), a is the particle radius, D_∞ is the diffusion coefficient (bulk value), Pe is the Peclet number, and V_h is the characteristic particle velocity due to flow.

It should be mentioned that in the case of gravity driven adsorption (sedimentation) Schaaf *et al.*⁸ defined the external force parameter in the form of the dimensionless particle radius R^* which is connected with ours through the relationship $R^* = Ex^{1/4}$.

Based on these definitions three limiting adsorption regimes can be distinguished:

- (i) $Ex \ll 1$ and $Pe \ll 1$,
- (ii) $Ex \gg 1$ and $Pe \ll 1$,
- (iii) $Ex = 0$ and $Pe \gg 1$.

The adsorption phenomena in case (i) seem to be well accounted for by the random sequential adsorption (RSA) model^{3,4,15,16} based on the assumption that particles are adsorbing sequentially and irreversibly at available surface areas of an homogeneous interface; when an adsorbing particle meets an area occupied by any preadsorbed particles it is rejected; the next adsorption attempt is entirely uncorrelated with any of the previous ones. An improvement of the RSA model consists in considering particle diffusion by means of either the approximate lattice model¹⁷ or the Brownian dynamics method.^{3,12} Hence, in this model, called diffusion random sequential adsorption (DRSA), the consecutive ad-

^{a)} Author to whom all correspondence should be addressed. Electronic mail: ncadamcz@cyf.-kr.edu.pl

sorption attempts are correlated with previous ones through the usual exponentially vanishing autocorrelation function. It was shown^{3,12,17} that both adsorption kinetics and the pair correlation function g_2 originating from the DRSA model deviate under transient conditions from their RSA counterparts. However, these deviations are not too significant and vanish when approaching the jamming concentrations of adsorbed particles which differ only marginally from each other.¹⁷

In case (ii) the ballistic model^{6–9,11,13,14} seems appropriate in which one assumes that adsorbing particles are not rejected when they approach preadsorbed particles but they follow the path of a steepest descent to find an uncovered area nearby where they can adsorb irreversibly. Both particle adsorption kinetics (hence the ASF) and the pair correlation function predicted by the ballistic model are essentially different in comparison with the RSA model.

On the other hand, for case (iii) the hydrodynamic adsorption (HA) model is valid^{3,10} characterized by increased surface blocking effects due to the coupling between shearing flows and repulsive electrostatic interactions. Hence the probability of particle adsorption in the downstream direction (behind the preadsorbed particle) becomes much lower than in the upstream direction (before preadsorbed particle). Due to the complexity of this situation no rigorous results have been derived yet. However, the sequential Brownian dynamic simulations and experimental measurements^{3,10} enabled one to formulate approximate models analogous to the RSA approach with a noncircular excluded area whose size increased with the flow shear rate.

Usually, in experimental works, the kinetic aspects of particle adsorption under the above-mentioned regimes were studied.^{3,10} Then, by differentiating the surface concentration versus time dependencies one can in principle determine the ASF which is rather tedious procedure, however.

It was, therefore, suggested recently^{8,9} that the ASF can alternatively be determined in a convenient way by studying fluctuations in surface concentration of particles adsorbed at various areas over homogeneous interfaces. The magnitude of these fluctuations is characterized by the reduced variance $\bar{V}r = \sigma^2 / \langle N_p \rangle = (\langle N_p^2 \rangle - \langle N_p \rangle^2) / \langle N_p \rangle$ (where N_p is the number of particles found over a given surface area and $\langle \rangle$ denotes the usual averaging procedure). Then, using the recent results of Schaaf *et al.*^{8,9} one can calculate ASF from the general relationship

$$\phi = \bar{V}r, \quad (1)$$

valid for all the above transport mechanisms in the limit of low and moderate surface concentrations.

This result has been confirmed using a different approach based on the approximate solution of the master equation.¹⁸ It was demonstrated that in the low concentration limit $\bar{V}r = \phi = 1 - C_1 \bar{\theta}$ for the RSA and the hydrodynamic models ($\bar{\theta} = \pi a^2 \langle N_p \rangle / S$ is the dimensionless surface concentration, a is the particle radius, S is the surface area of the interface). The C_1 constant characterizes the nonequilibrium interactions between adsorbing and adsorbed particles. It can be determined experimentally by measuring $\bar{V}r$ as a function

of $\bar{\theta}$. Hence, by studying fluctuations one can gain important clues about interactions among adsorbing and adsorbed particles under dynamic conditions.³

It should be noted that the variance $\bar{V}r$ can be determined either directly by counting the number of particles adsorbed on many equal sized areas or via the universal relationship valid for reversible and irreversible systems,¹⁹

$$\bar{V}r = \sigma^2 / \langle N_p \rangle = 1 + 2\bar{\theta} \int_0^\infty [g_2(\bar{r}) - 1] \bar{r} d\bar{r}, \quad (2)$$

where g_2 is the two-dimensional (2D) pair correlation function (radial distribution function) and $\bar{r} = r/a$ is the dimensionless radial distance.

As discussed in Ref. 14 the integration procedure may become inaccurate, however, especially for low $\bar{\theta}$ when the accuracy of determining g_2 at large separations becomes rather low. Another difficulty is associated with a proper experimental determination of the averaged surface concentration $\bar{\theta}$ involving a knowledge of the averaged particle radius a . It was recently demonstrated²⁰ that even for systems characterized by low polydispersity (a standard deviation of about 10%) the averaged size of adsorbed particles deviates significantly from that characteristic for the bulk population. This may cause severe problems with the convergence of the integral on the right-hand side of Eq. (2).

The validity of Eq. (2) has been confirmed experimentally^{11,13,14} using noninteracting polymeric particles of micrometer size range and density 1.5 g/cm³, i.e., under experimental conditions corresponding to the ballistic model when $Ex \gg 1$. Similar experiments performed for lower density polystyrene particles (1.055 g/cm³)¹⁴ revealed quite unexpectedly that also in this case (when $Ex \ll 1$), the variance of the concentration fluctuations was very similar to the ballistic model predictions, i.e., much larger than that predicted by the RSA model.

To our knowledge there is no experimental evidence concerning fluctuation in irreversible systems of interacting particles under the RSA and HA adsorption regimes. This should be the goal of our paper. The fluctuations in particle surface concentration shall be studied via the direct observation techniques using model colloid microparticles and the impinging-jet cells.³

It seems that our results obtained for model colloid systems characterized by high monodispersity and well-defined surface properties, can be used for predicting adsorption and fluctuation phenomena in molecular systems for which direct experimental measurements are not feasible.

II. EXPERIMENT

A. The experimental cell

Particle adsorption experiments were performed *in situ* using the direct microscope observation method and the slot-jet flow cell shown schematically in Fig. 1. The cell consisted of the internal rectangular channel A (dimensions 0.082 per 1.6 cm) through which the particle suspension was driven due to the hydrostatic pressure difference (changeable within broad limits). The pressure gradient in the channel

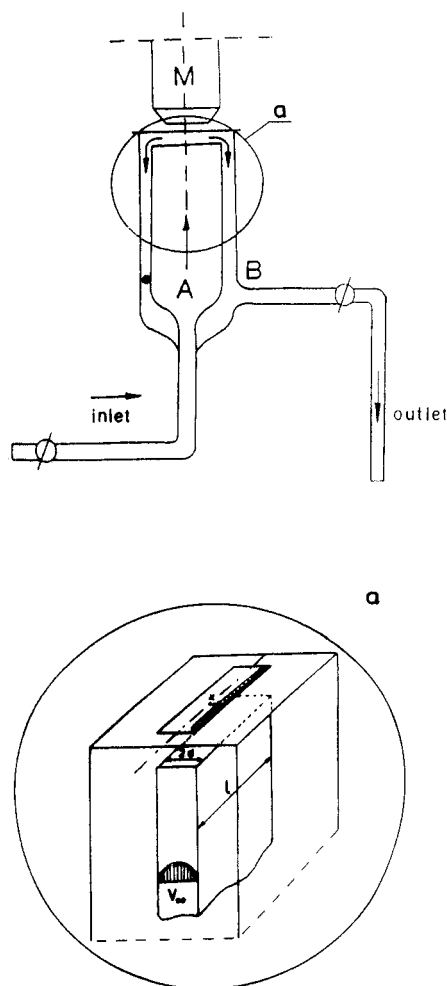


FIG. 1. The experimental cell used for the *in situ* observations of particle adsorption from the slot impinging jet.

determined the volumetric flow rate Q which was kept constant during an experiment. The suspension stream formed at the slot of the inside channel impinged against the perpendicularly oriented mica sheet held fixed to the external channel B due to under-pressure prevailing in the cell (hence no contaminating substance was used to seal the cell). Then the suspension left the external channel and was discarded. For the diffusion controlled adsorption experiments a circular impinging jet cell (type "b") was also used in order to reduce the suspension consumption. Further details of the cell operation were described in our previous papers.^{10,12,18}

The particle adsorption process was observed in real time using the Leitz optical microscope (dark-field illumination) coupled with a charge-coupled device TV camera (Hamamatsu type C-3077), an image processor (Argus10 type C-3930 Hamamatsu), and video recorder (VHS Panasonic type AG-7350).

B. Materials and methods

In our experiments we used model suspensions of polystyrene latex particles of micron size range and narrow size distributions.

The suspensions of negatively charged polystyrene latex was synthesized according to the polymerization procedure described in Ref. 21. The sample obtained from the polymerization was purified by steam distillation and washed on a Sartorius membrane filter until the filtrate conductivity stabilized around the value of pure water (about $1\text{--}2\ \mu\text{S}$). The pH of the samples measured before and after each experiment was usually 5.6–6.

Two latex samples having an average particle size of 0.88 and $1.0\ \mu\text{m}$ and standard deviation of 6% (as determined by the Coulter counter) were used in the experiments. Due to the low specific density of these latexes equal $1.05\ \text{g/cm}^3$ the suspension sedimentation effects were practically eliminated. The zeta potential of the latex particles (measured by a zeta sizer) was $-50\ \text{mV}$ for the ionic strength prevailing in our experiments ($10^{-4}\ \text{M}$ fixed by using high purity solutions of KCl).

As the adsorbing surface we used molecularly smooth mica sheets supplied by Mica & Micanite Supplies Ltd. England. In order to ensure localized and irreversible adsorption of negatively charged polystyrene particles the natural negative charge of mica was converted to a positive one. This was accomplished by bringing freshly cleaved mica sheets in contact with a 1% aqueous solution of *N*-[3-(trimethoxy silyl) propyl]-ethylene diamine. Then the sheets were washed and heated for 24 h at $80\ ^\circ\text{C}$.

In due course the term modified mica shall be used for mica sheets prepared according to the above procedure.

The particle adsorption experiments were performed by flowing the colloid suspension through the cell for a given time (usually 2–8 h depending on the bulk suspension concentration) until a prescribed surface concentration was attained. The signal resulting from the digital TV camera was continuously recorded. After finishing the adsorption experiment the statistical analysis of the distribution of adsorbed particles was performed. Equal-sized surface areas ΔS were chosen at random at the interface and the number of adsorbed particles on each area was determined using the image freeze option. Usually, 200–300 nonoverlapping areas were considered. The size of the surface element ΔS was adjusted to the surface concentrations in such a way that the average number of particles adsorbed equaled 40–50. The subsequent variance analysis and histogram plotting was done automatically using special computer programs.

The pair correlation function determination requiring higher accuracy was performed using the micrograph technique combined with the magnetic digitizer.^{18,22} Using this method one can measure the x, y coordinates of individual adsorbed particles with a precision of $0.1\ \text{mm}$ (the entire picture size being about $40 \times 30\ \text{cm}$). Then these coordinates were processed in the usual way described elsewhere.³ The number of particles per one picture used for g_2 determination ranged from 300 to 1000 depending on the surface concentration of adsorbed particles. In order to attain a sufficient accuracy of g_2 the information from about ten various pictures was averaged.

III. RESULTS AND DISCUSSION

A. Determining the pair correlation function

As was mentioned, the case of external force dominated adsorption (governed by the ballistic model) was fairly well studied in the literature.^{8,9,11,13,14} Therefore, we focused our attention on the diffusion and flow controlled adsorption mechanisms, i.e., on cases (i) and (iii) defined in Sec. I. Selecting the tangential liquid velocity as the characteristic scaling variable one can define the Pe number for our experimental cell of type “a” and “b” as¹⁰

$$\begin{aligned} \text{Pe}_{\parallel} &= 2\alpha_s(\text{Re}) \frac{V_m a^2 x}{d^2 D_{\infty}}, & \text{Re} &= \frac{V_m d}{\nu}, & V_m &= Q/2dl, \\ \text{Pe}_{\parallel} &= 2\alpha_r(\text{Re}) \frac{V_m a^2 r}{R^2 D_{\infty}}, & \text{Re} &= \frac{V_m R}{\nu}, & V_m &= Q/\pi R^2, \end{aligned} \quad (3)$$

where α_s and α_r are the dimensionless functions of the Reynolds number Re , V_m is the mean fluid velocity, x and r are the distances from the cell center, d is the width and l the length of the slot of cell a (Fig. 1), R is the radius of the aperture in cell b. The functions α_s and α_r were of the order of unity for our experimental conditions ($\text{Re} < 20$).

All our experiments reported hereafter were characterized by two different values of Pe_{\parallel} , i.e., $\text{Pe}_{\parallel} = 1$ and $\text{Pe}_{\parallel} = 100$ when the RSA and the hydrodynamic adsorption (HA) models were expected to be valid, respectively (in our previous work¹⁰ we used \bar{G} instead of Pe_{\parallel}). As mentioned, the ionic strength in both series of experiments was equal to 10^{-4} M which prevented particle aggregation likely to occur for $I > 10^{-3}$ M. The Debye screening length $\text{Le} = (\epsilon kT/8\pi e^2 I)$ for this ionic strength value was equal 300 \AA , i.e., about 0.06 particle radius. Since the electrostatic interactions remain important over distances of $2-3 \text{ Le}$ ^{3,23} one can expect that they should play a significant role in our experimental system. This enabled us, therefore, to determine fluctuation phenomena of interacting (soft) particles in contrast with previous studies concerned with hard particles alone.^{8,9,11,13,14}

It should, however, be mentioned that the existing theoretical approaches describing fluctuations are only valid for homogeneous systems with no macroscopic surface concentration gradient. We have, therefore, carried out our experiments in such a way that this prerequisite was fulfilled. For the diffusion controlled adsorption regime, i.e., case (i), this is a simple task since the entire surface area is uniformly accessible for adsorbing particles as predicted theoretically.³ This has been confirmed for various experimental conditions by measuring the averaged particle surface concentration as a function of the distance from the symmetry plane of the experimental cell.

A more complicated situation arises for the flow dominated adsorption regime when indeed the surface concentration decreases monotonically when proceeding in the direction perpendicular to the symmetry plane (x axis). The characteristic length scale of this variation is of the order of $100 \text{ }\mu\text{m}$. However, the concentration gradient vanishes when proceeding in the direction parallel to the symmetry plane (y axis). Thus, in order to minimize the effect of the surface

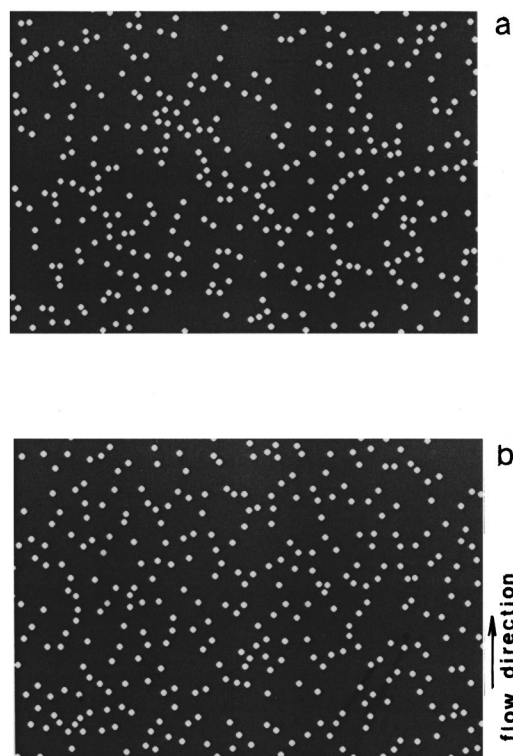


FIG. 2. The micrographs showing polystyrene particles adsorbed at mica surface: (a) for the RSA mechanism $\text{Pe}_{\parallel} = 1$, $\bar{\theta} = 6.5\%$; (b) for the HA mechanism, $\text{Pe}_{\parallel} = 100$, $\bar{\theta} = 6.25\%$.

concentration gradient we confined our experiments to the thin rectangular surface area (shadowed in Fig. 1) having the typical dimensions of 40 per $5000 \text{ }\mu\text{m}$. It has been confirmed in separate experiments that $\langle N_p \rangle$ was statistically independent of the position within this surface element.

This can also be qualitatively observed in Figs. 2(a) and 2(b) showing the micrographs of polystyrene latex particles adsorbed at mica under the RSA and HA regimes, respectively. The averaged surface concentration (two-dimensional density) $\bar{\theta}$ at which the photographs were taken was about 6% .

The particle distributions shown in Figs. 2(a) and 2(b) can quantitatively be characterized in terms of the pair correlation function g_2 plotted in Figs. 3. The lines in Figs. 3(a) and 3(b) represent the Boltzmann distribution, i.e., $g_2 = \exp(-E(\bar{r})/kT)$ (where E is the interaction energy and $\bar{r} = r_{12}/a$ is the dimensionless distance between particle centers, r_{12} is the distance between their centers. It was shown^{3,22} that the net interaction energy in our system is determined by the screened electrostatic interaction energy given by the Yukawa type potential

$$E(\bar{r}) = \frac{E_0}{\bar{r}} e^{-(a/\text{Le})(\bar{r}-2)}, \quad (4)$$

where $E_0 = 8\epsilon a(kT/e)^2 \text{th}^2(\psi^0 e/4kT)$ is the interaction energy at contact and ψ^0 is the surface potential of the particle.

As can be seen in Fig. 3(a) for the RSA model the experimental pair correlation function is well described by the

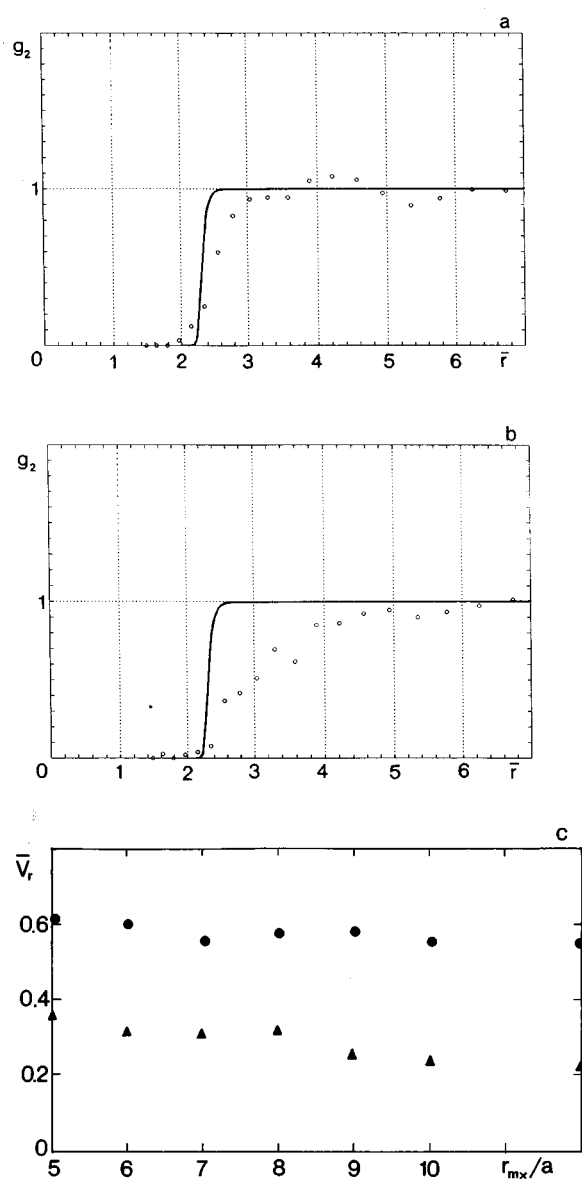


FIG. 3. The pair correlation function g_2 : (a) for the RSA, $Pe_{||}=1$, $\bar{\theta}=6.1\%$; (b) for HA, $Pe_{||}=100$, $\bar{\theta}=5.8\%$. The points are the experimental results obtained for $I=10^{-4}$ M and the lines denote the Boltzmann distribution, i.e., $g_2 = e^{-E(\bar{r})/kT}$; (c) the dependence of the reduced variance \bar{V}_r calculated by integrating the pair correlation functions shown in (a) (circles) and in (b) (triangles).

Boltzmann distribution. The nonvanishing part of g_2 observed for $\bar{r} < 2$ in Fig. 3(a) can be attributed to the slight polydispersity effect as discussed in Ref. 20.

On the other hand, for the HA model the experimental values of g_2 deviate considerably from the Boltzmann distribution and the region where g_2 assumes values significantly smaller than one is comparable with particle dimensions. This indicates unequivocally that in the case of irreversible adsorption the flow affected considerably the g_2 function (hence the structure of the adsorbed layer). This agrees with previous results of Sjollesma and Busscher²⁴ who studied particle adsorption in a parallel-plate channel. As was mentioned, this can be explained in terms of the hydrodynamic

scattering effect¹⁰ caused by the coupling between the shearing hydrodynamic flows and the electrostatic double-layer interactions. Since in our work we are primarily interested in the fluctuation of particle number density these aspects of HA are not discussed. Further details can be found in a review paper.³

Knowing g_2 one can attempt to determine \bar{V}_r from Eq. (2) as was done previously in Refs. 11, 13, and 14. Obviously, under any real situation the upper integration limit r_{mx} must remain finite. Then, it should be proven that the definite integral occurring in Eq. (2) approaches asymptotically a constant value when increasing r_{mx} . As pointed out in Ref. 14 due to the limited accuracy of determining the averaged value of $\bar{\theta}$ the integral may diverge in this limit, especially for low coverages.

Therefore, in our calculations we adopted another procedure of calculating \bar{V}_r , i.e., the g_2 functions obtained for individual pictures were first integrated and then averaged over an ensemble of pictures for which $\bar{\theta}$ was very similar but not identical. It seems that our procedure is convergent because the averaged \bar{V}_r value is rather insensitive to the upper integration limit as can be seen in Fig. 3(c). However, for r_{mx}/a larger than 10 the accuracy of \bar{V}_r determination is decreased due to the decreasing number of particles considered (since particles adsorbed at the distance smaller than r_{mx} from the perimeter of a given picture were not counted).

Considering the dependencies shown in Fig. 3(c) one can estimate that the averaged value of \bar{V}_r was 0.58 for the RSA model ($\bar{\theta}=6.1\%$) and 0.30 for the HA model ($\bar{\theta}=5.8\%$). This result confirms quantitatively the conclusion that the fluctuations in particle density are considerably diminished in the systems where adsorption is influenced by hydrodynamic interactions.

Since the calculation of \bar{V}_r by integrating the pair correlation function according to Eq. (2) is rather tedious we attempted to use the alternative direct route via the variance analysis of experimental histograms.

B. Fluctuation in the number of adsorbed particles

Let us consider a small surface element ΔS chosen randomly at the adsorption plane whose overall surface area is equal to S . We assume that $\Delta S \ll S$ which can be easily realized experimentally. Denote by N_p the number of particles adsorbed at ΔS after the time t . Because particle adsorption is a stochastic process the value of N_p is a statistical variable changing from one surface element to another. Thus, the interface with adsorbed particles corresponds to a frozen fluctuation more convenient to study than the particle density fluctuations occurring in the bulk. For an uncorrelated sequence of single particle adsorption events (as is the case for low surface concentrations) the probability of finding exactly N_p particles on ΔS is given by the binomial distribution

$$q(N_p, M) = \binom{M}{N_p} \left(\frac{\Delta S}{S} \right)^{N_p} \left(1 - \frac{\Delta S}{S} \right)^{M-N_p}, \quad (5)$$

where

$$\binom{M}{N_p} = \frac{M!}{(M-N_p)!N_p!}$$

is the number of combinations for which particle configuration remains unchanged (undistinguishable particles) and M is the total number of elementary adsorption events.

Considering that in our case $M \gg N_p$ and remembering that the averaged value of N_p is given by $\langle N_p \rangle \cong \Delta S M / S$ one can derive from Eq. (5) the well-known Poisson distribution law

$$p(N_p) = \frac{\langle N_p \rangle^{N_p}}{N_p!} \left(1 - \frac{\langle N_p \rangle}{M} \right)^{M-N_p} \cong \frac{\langle N_p \rangle^{N_p}}{N_p!} e^{-\langle N_p \rangle}. \quad (6)$$

Moreover, it can be shown by using the Stirling formula that for $\langle N_p \rangle > 30$, Eq. (6) can well be approximated by the Gauss distribution, i.e.,

$$p(N_p) = \frac{1}{\sqrt{2\pi\langle N_p \rangle}} \exp\left(-\frac{1}{2} \frac{(N_p - \langle N_p \rangle)^2}{\langle N_p \rangle}\right). \quad (7)$$

Note that the reduced variance $\bar{V}r$ for both distributions expressed by Eqs. (6) and (7) is equal one.

As mentioned above the Poisson distribution is expected to describe well the situation when the probability of successive adsorption events remains independent of the number of particles already present on the surface. It is obvious that this condition is violated for concentrated colloid systems as a result of excluded volume effects and interactions between adsorbed and adsorbing particles.

Thus, for interacting particles Wojtaszczyk *et al.*¹¹ have formulated and solved numerically (via a recursion procedure) the master equation describing the evolution of probability as a function of N_p and M . Their numerical calculations obtained by adopting the mean field approximation are, however, as complicated as the original RSA simulations from which the fluctuations can be calculated more directly.

On the other hand, it was shown in Ref. 18 that in the limit of large $\langle N_p \rangle$ adsorption probability over ΔS becomes proportional to $\prod_{i=1}^{N_p} \phi_i(N_p)$ and one can express the distribution of N_p by the modified Gauss law

$$p(N_p) = \frac{1}{\sqrt{2\pi\langle N_p \rangle \bar{V}r}} \exp\left(-\frac{1}{2} \frac{(N_p - \langle N_p \rangle)^2}{\langle N_p \rangle \bar{V}r}\right) \quad (8)$$

with $\bar{V}r$ connected with the ASF thorough the explicit analytical dependence

$$\bar{V}r(\bar{\theta}) = \left(\frac{\phi(\bar{\theta})}{\phi(\bar{\theta}) - \bar{\theta} \frac{d\phi}{d\bar{\theta}}} \right)_{\bar{\theta}=\bar{\theta}}, \quad (9)$$

where $\bar{\theta} = \pi a^2 \langle N_p \rangle / \Delta S$ is the averaged surface concentration of adsorbed particles.

For repulsive interaction potential, e.g., that described by Eq. (4), $d\phi/d\bar{\theta} < 0$ and the value of $\bar{V}r$ is always smaller than one, i.e., the value characteristic for the Poisson distribution.

In other words, the probability of finding large relative fluctuations for higher concentrations becomes much smaller than in dilute systems in which the excluded volume effects play a minor role.

It was shown previously^{4,5,8,9} that the ASF function can often be expressed in terms of the power series expansion

$$\phi = 1 - \sum C_n \theta^n. \quad (10)$$

Then, differentiating this dependence and substituting into Eq. (9) one can derive for $\bar{V}r$ the analytical expression

$$\bar{V}r = \frac{1 - \sum C_n \theta^n}{1 - \sum (n-1) C_n \theta^n}. \quad (11)$$

For the RSA model the constants C_1 – C_3 were calculated analytically by Schaaf and Talbot.⁴ On the other hand, it can be shown using the effective hard particle concept that for particles interacting via the Yukawa potential these coefficients can be approximated by the expressions²⁵

$$\begin{aligned} C_1 &= 4(1 + H^*)^2, \\ C_2 &= \frac{6\sqrt{3}}{\pi} (1 + H^*)^4, \end{aligned} \quad (12)$$

$$C_3 = 1.407(1 + H^*)^6,$$

where H^* is the effective interaction range given by²⁶

$$H^* = \frac{\text{Le}}{2a} \ln(E_0/E_{\text{ch}}). \quad (13)$$

E_{ch} is the characteristic interaction energy, assumed usually to lie within the limits 1.5–2 kT units.

Obviously, for $H^* \rightarrow 0$ the constants C_1 – C_3 reduce to that derived by Schaaf and Talbot⁴ for hard spheres.

Moreover, it was shown in Ref. 10 that the series expansion can approximate the ASF for the hydrodynamic adsorption model as well with the constants C_1 – C_2 given by

$$\begin{aligned} C_1 &= \frac{4 \left(1 - \frac{1}{\sqrt{2}} \right)}{\theta_{\text{st}}}, \\ C_2 &= \frac{1}{8} C_1^2, \end{aligned} \quad (14)$$

where θ_{st} is the stationary surface concentration which for large Pe becomes C_h/Pe (where C_h is a dimensionless constant equal 0.06¹⁰).

Knowing that $C_1 \neq 0$ for the RSA and HA models one can deduce from Eq. (11) that in the limit of low density the reduced variance is given by the simple expression

$$\bar{V}r = 1 - C_1 \bar{\theta} = \phi(\bar{\theta}). \quad (15)$$

This agrees with the results of Schaaf *et al.*⁸

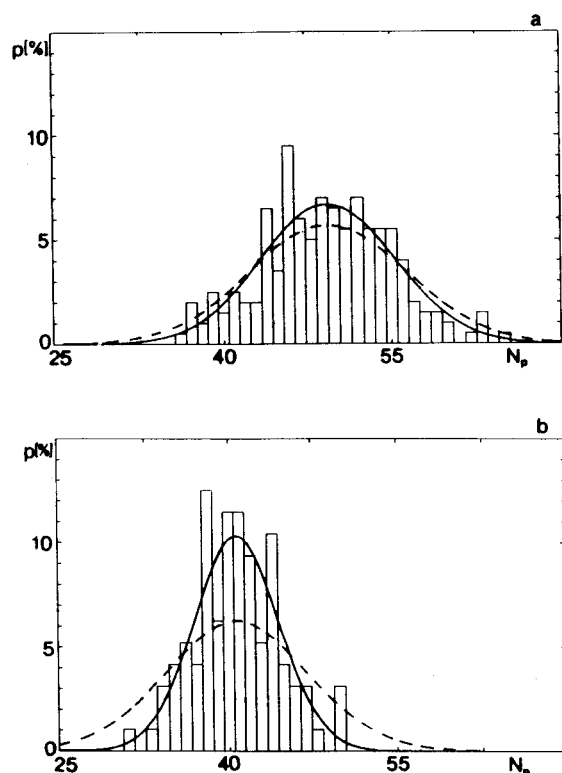


FIG. 4. The histograms showing the probability of finding a surface area with adsorbed N_p particles: (a) for the RSA, $Pe_{II}=1$, $\bar{\theta}=5.6\%$, $\langle N_p \rangle=49.3$, $\bar{V}r=0.72$; (b) for the HA, $Pe_{II}=100$, $\bar{\theta}=5.27\%$, $\langle N_p \rangle=40.7$, $\bar{V}r=0.37$. The continuous lines show the modified Gauss distribution calculated from Eq. (8) and the broken line shows the results calculated from Eq. (8) by assuming $\bar{V}r=1$ (low density limit).

Equation (15) has considerable practical significance because it indicates that by measuring fluctuations in particle density (for low θ) one can determine the C_1 constant which has a natural physical interpretation as the averaged surface area excluded by one particle. This in turn enables one not only to estimate the range of interaction between adsorbed and adsorbing particles but also adsorption kinetics for low coverages. Such determination of C_1 is especially important in systems where adsorption is influenced by flow for which theoretical prediction of ϕ is cumbersome.¹⁰

Thus, the goal of this part of our work was to verify the range of validity of Eqs. (9)–(15) for a theoretical interpretation of fluctuations in irreversible systems.

The experimentally measured histograms showing the probability of finding a surface area with adsorbed N_p particles are presented in Fig. 4 for both the RSA and the HA regimes at practically equal surface concentration of about 6%. The averaged value of N_p in these experiments was about 40 which assures that the discrete histograms can well be approximated by the quasicontinuous probability distributions given by Eq. (8). The reduced variance $\bar{V}r = \langle N_p^2 \rangle - \langle N_p \rangle^2$ determined from these histograms was equal to 0.72 and 0.37 for the RSA and HA regimes, respectively. These values are slightly larger than those calculated previously by integration of the pair correlation function according to Eq. (2). In this respect our results agree well with

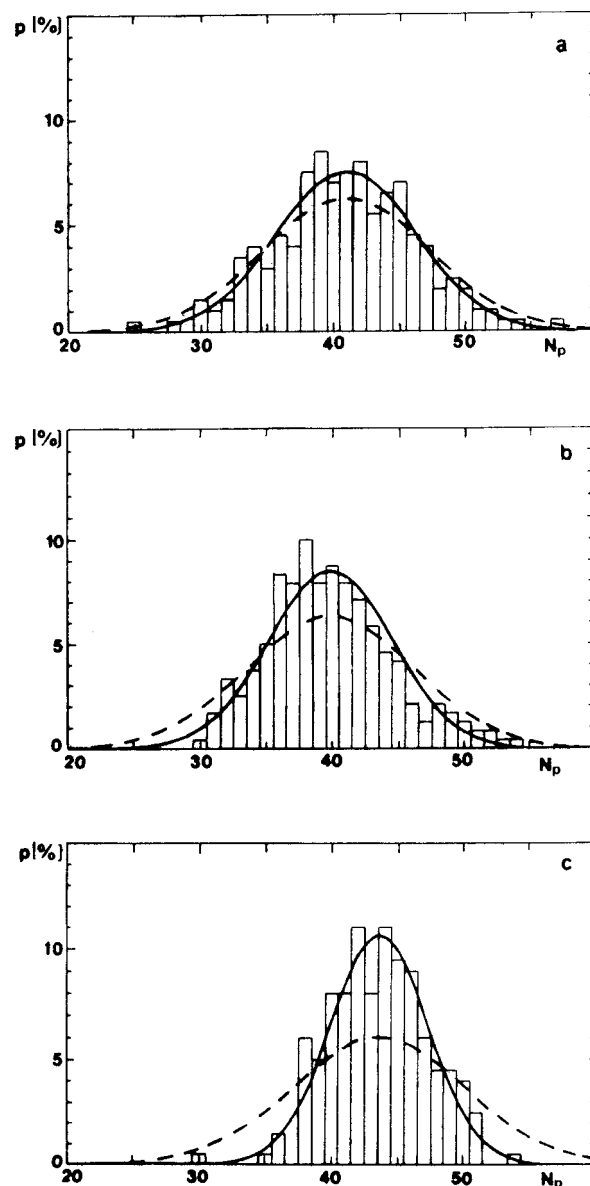


FIG. 5. The sequence of histograms determined experimentally for various $\bar{\theta}$ in the case of the RSA mechanism: (a) $\bar{\theta}=9.2\%$, $\langle N_p \rangle=40.9$, $\bar{V}r=0.69$; (b) $\bar{\theta}=13.4\%$, $\langle N_p \rangle=39.8$, $\bar{V}r=0.55$; (c) $\bar{\theta}=23.6\%$, $\langle N_p \rangle=43.6$, $\bar{V}r=0.32$. The continuous lines are the theoretical prediction calculated from Eq. (8) and the broken lines denote the low density limiting Gauss distributions.

previous ones obtained in the case of gravity driven adsorption.¹⁴

As can be seen in Fig. 4 the modified Gauss distribution given by Eq. (8) reflects well the experimental histograms for both adsorption regimes. This is also the case for higher surface concentrations as well which can be observed in Fig. 5 for the RSA model and $\bar{\theta}=9.2\%$, 15% , and 23.6% (such surface concentrations are not accessible within the HA regime, due to the low stationary value of $\theta_{st}=6.5\%$). It can be seen in Fig. 5 that the distributions become narrower for increasing values of the surface concentration which is reflected well by the decrease of the relative variance $\bar{V}r$ from 0.69 (for $\bar{\theta}=9.2\%$) to 0.32 (for $\bar{\theta}=23.6\%$). Thus, for increasing $\bar{\theta}$ the fluctuations in particle surface concentration

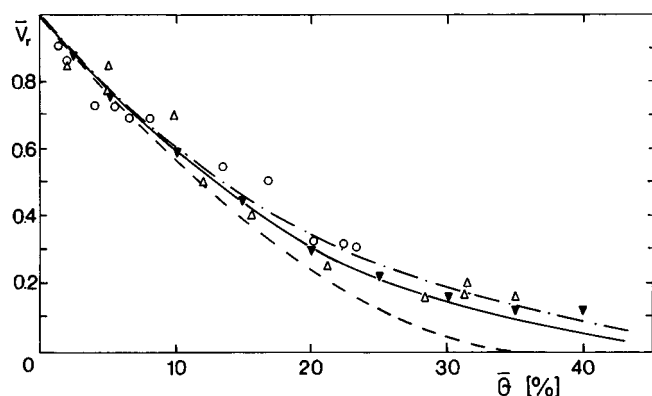


FIG. 6. The reduced variance $\bar{V}r$ as a function of $\bar{\theta}$. RSA regime, $I=10^{-4}$ M. The points \circ , Δ denote experimental results and the \blacktriangledown points show the computer simulations. The continuous line represents the theoretical results calculated from Eqs. (10) to (11), the broken line from the Schaaf *et al.* (Ref. 8) equation $\bar{V}r=\phi$, and the --- line from the equilibrium scaled particle theory [Eq. (19)].

around the mean value are considerably decreased due to the surface exclusion effects.

The analysis of experimental histograms illustrating directly fluctuations in concentration of adsorbed particles is rather cumbersome for a quantitative determination of the ASF function.

More information concerning $\phi(\bar{\theta})$ can be gained when determining $\bar{V}r$ for various surface concentrations and then plotting the results obtained in the form of the $\bar{V}r$ vs $\bar{\theta}$ dependence. This is done in Fig. 6 for the RSA model (experiments performed both in cell a and b) and $\bar{\theta}$ ranging from 1% to 35%. For comparison the results stemming from the computer “experiments” performed according to the RSA simulation scheme are also plotted in Fig. 6. As can be seen they correlate very well with the experimental points for the entire range of the surface concentration studied. Note also that the experimental results are well reflected by the analytical prediction stemming from Eq. (11) [with the C_1-C_3 constants calculated from Eq. (12)]. The slight positive deviation of experimental points from theoretical predictions observed for $\bar{\theta}>30\%$ can be attributed to the inadequacy of the mean field approximation for large surface concentration. Hence, the variance does not decrease to zero as Eq. (11) suggests but attains a residual value of about 0.1 due to fluctuations in particle distribution over ΔS for a given constant N_p value. On the other hand, the theoretical results of Schaaf *et al.*,⁸ i.e., $\bar{V}r=\phi$ (the broken line in Fig. 6) are only applicable for $\bar{\theta}<20\%$.

The good agreement of the theoretical and experimental results furnishes further arguments in support of the effective hard particle concept [expressed by Eqs. (12)–(14)].

Since in many theoretical works^{4,5} it has been postulated that the irreversible adsorption processes governed by the RSA mechanism become identical with reversible adsorption in the low density limit we attempted to test this hypothesis. Thus, our experimental results, which agreed well with the RSA model as mentioned above, were compared with theoretical predictions derived on the basis of statistical-

mechanical theory of equilibrium hard-sphere fluid using the known thermodynamic relationship²⁷ (applied for a 2D system of adsorbed molecules)

$$\bar{V}r = \frac{kT}{S_1} \bar{\theta} \kappa_s = 1 + 2\bar{\theta} \int_0^\infty [g_2(\bar{r}) - 1] \bar{r} d\bar{r}, \quad (16)$$

where

$$\kappa_s = -\frac{1}{S} \left(\frac{\partial S}{\partial p} \right)_{\bar{N}_p, T} = \frac{1}{\bar{\theta}} \left(\frac{\partial p}{\partial \bar{\theta}} \right)_{\bar{N}_p, T}^{-1}. \quad (17)$$

$S_1 = \pi a^2$ is the surface area of one molecule, S is the surface area of the entire system, and p is the 2D pressure in the adsorbed molecule layer. The expression for the pressure can be calculated from the scaled-particle theory²⁷ which predicts the analytical expression

$$p = \frac{kT}{S_1} \frac{\bar{\theta}}{(1 - \bar{\theta})^2}. \quad (18)$$

Taking a derivative of this dependence and substituting into Eq. (16) gives for $\bar{V}r$ the simple expression

$$\bar{V}r = \frac{(1 - \bar{\theta})^3}{1 + \bar{\theta}}. \quad (19)$$

This formula is valid for noninteracting particles and proved rather inaccurate for our system. However, the discrepancy can be considerably reduced when the effective surface concentration:

$$\bar{\theta}^* = \bar{\theta}(1 + H^*)^2$$

is substituted into Eq. (19). As can be observed in Fig. 6 the agreement between the experimental results and theoretical predictions calculated from Eq. (19) using the effective surface concentration is satisfactory for the entire range of $\bar{\theta}$. This may suggest that by introducing the effective particle radius (or effective surface concentration) one can use the known formulas derived from the statistical-mechanical approaches to describe the fluctuation phenomena in irreversible systems governed by the RSA mechanism. Our results seem, therefore, to confirm the theoretical prediction formulated in the previous works.^{4,5}

The irreversibility effect plays a significant role, however, for the HA regimes. This can be clearly seen in Fig. 7 where the dependence of $\bar{V}r$ on $\bar{\theta}$ is shown for $Pe_0=100$. In accordance with previous results derived by integrating the g_2 function the values of $\bar{V}r$ for the same $\bar{\theta}$ are smaller under the HA in comparison with the RSA regime. Thus, the RSA or the scaled particle equilibrium results [calculated from Eq. (19)] describe poorly the experimental measurements.

However, Eq. (9) still can successfully be used with the coefficients of the series expansion of ϕ calculated from Eq. (14). Due to the fact that $\bar{\theta}<6\%$ the quadratic term has little effect on $\bar{V}r$ and Eq. (15) is applicable. As can be observed in Fig. 7, Eq. (15) can indeed be used for predicting the dependence of $\bar{V}r$ on $\bar{\theta}$. As expected for $\bar{\theta}>5\%$ small positive deviations from the theoretical results can be observed in

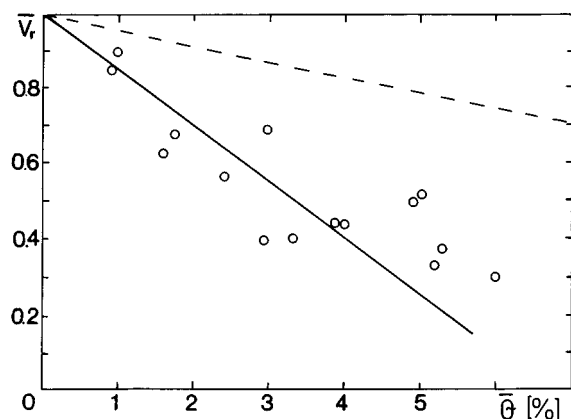


FIG. 7. The dependence of $\bar{V}r$ on $\bar{\theta}$ for the HA regime, $I=10^{-4}$ M. The continuous line denotes the theoretical results calculated from Eq. (15) and the broken line from Eq. (19).

Fig. 7. It seems that in order to fully account for the fluctuations occurring under HA regimes one should perform Brownian dynamic type simulations of particle adsorption. Due to the lack of appropriate hydrodynamic resistance tensors for multiparticle systems such calculations cannot be performed at present with a sufficient accuracy.

Comparison of the results shown in Figs. 6 and 7 confirms the thesis mentioned in Sec. I that for irreversible adsorption of colloid particles the density fluctuations are not uniquely characterized in terms of $\bar{\theta}$ alone as is the case for equilibrium systems.

IV. CONCLUDING REMARKS

The experimental cells based on the impinging-jet principle were proven useful for direct, quantitative studies of fluctuation phenomena occurring during irreversible adsorption of colloid particles.

Due to the surface exclusion effects the magnitude of statistical fluctuations was found to decrease monotonically with the increase in the surface concentration of adsorbed particles. These fluctuations can be described for larger $\langle N_p \rangle$ by the quasicontinuous Gauss distribution [Eq. (8)] derived by assuming the mean field approximation. The relative variance of the distribution is given by

$$\bar{V}r = \sigma^2 / \langle N_p \rangle = \left(\frac{\phi(\theta)}{\phi(\theta) - \theta \left(\frac{d\phi}{d\theta} \right)} \right)_{\theta=\bar{\theta}}.$$

The ASF function occurring in this equation can be approximated by the power series expansion with the coefficients calculated using the effective interaction range concept. For $\bar{\theta} > 30\%$ this formula breaks down, however, and the residual fluctuations (with $\bar{V}r$ about 0.1) can only be described by numerical simulations.

The experiments performed under the RSA regime indicate that the concept of the effective interaction range can also be used for rescaling the known statistical-mechanical theories developed for reversible systems. Thus the equation

describing concentration fluctuations in the grand canonical ensemble can be used for determining $\bar{V}r$ in our irreversible colloid systems, i.e.,

$$\bar{V}r = \frac{(1 - \bar{\theta}^*)^3}{1 + \bar{\theta}^*}$$

with $\bar{\theta}^* = \bar{\theta}(1 + H^*)^2$.

It was found, however, that in contrast to equilibrium systems, the fluctuations are not uniquely characterized in terms of $\bar{\theta}$ alone but they also depend on the transport mechanism of particles to surfaces. Hence for the hydrodynamic adsorption regime the reduced variance is much lower (for the same $\bar{\theta}$) due to the hydrodynamic scattering effects. This can also be accounted for by using the series expansion of the ASF functions.

Since it was shown in accordance with previous results of Schaaf *et al.*⁸ that $\bar{V}r = \phi$ for low surface concentrations, the $\bar{V}r$ measurements can be used to predict the ASF function in irreversible systems, especially to determine directly the effective surface area blocked by one particle. In this way adsorption kinetics of colloid particles can be estimated in a simple way.

It also seems that our results can be extrapolated to predict fluctuations and ASF functions in the case of adsorption of nonspherical particles (e.g., of spheroidal shape). This can have large practical significance in various studies of protein or bacteria adsorption whose shapes deviate usually from a spherical one.

ACKNOWLEDGMENTS

This work was partly supported by the KBN Grant No. 2 T09A 083 10. The authors are indebted to P. Weroński for performing the RSA simulations.

- ¹J. Feder and T. Giaever, *J. Colloid Interface Sci.* **78**, 144 (1980).
- ²J. J. Ramsden, *Phys. Rev. Lett.* **71**, 295 (1993).
- ³Z. Adamczyk, B. Siwek, M. Zembala, and P. Belouschek, *Adv. Colloid Interface Sci.* **48**, 151 (1994).
- ⁴P. Schaaf and J. Talbot, *J. Chem. Phys.* **91**, 4401 (1989).
- ⁵G. Tarjus, P. Schaaf, and J. Talbot, *J. Stat. Phys.* **63**, 167 (1991).
- ⁶R. Jullien and P. Meakin, *J. Phys. A* **25**, L189 (1992).
- ⁷A. P. Thompson and E. D. Glandt, *Phys. Rev. A* **46**, 4639 (1992).
- ⁸P. Schaaf, P. Wojtaszczyk, E. K. Mann, B. Senger, J. C. Voegel, and D. Bedeaux, *J. Chem. Phys.* **102**, 5077 (1995).
- ⁹P. Schaaf, P. Wojtaszczyk, B. Senger, J. C. Voegel, and H. Reiss, *Phys. Rev. E* **51**, 4292 (1995).
- ¹⁰Z. Adamczyk, B. Siwek, and L. Szyk, *J. Colloid Interface Sci.* **174**, 130 (1995).
- ¹¹P. Wojtaszczyk, P. Schaaf, B. Senger, M. Zembala, and J. C. Voegel, *J. Chem. Phys.* **99**, 7198 (1993).
- ¹²Z. Adamczyk, B. Siwek, and M. Zembala, *Colloids Surf.* **76**, 115 (1993).
- ¹³E. K. Mann, P. Wojtaszczyk, B. Senger, J. C. Voegel, and P. Schaaf, *Europhys. Lett.* **30**, 261 (1995).
- ¹⁴P. Wojtaszczyk, E. K. Mann, B. Senger, J. C. Voegel, and P. Schaaf, *J. Chem. Phys.* **103**, 8285 (1995).
- ¹⁵E. L. Hinrichsen, J. Feder, and T. Jossang, *J. Stat. Phys.* **44**, 793 (1993).
- ¹⁶J. W. Evans, *Rev. Mod. Phys.* **65**, 1281 (1993).
- ¹⁷B. Senger, P. Schaaf, J. C. Voegel, A. Johnner, A. Schmitt, and J. Talbot, *J. Chem. Phys.* **97**, 3813 (1992).
- ¹⁸Z. Adamczyk and L. Szyk, *Bull. Pol. Ac. Chem.* **43**, 243 (1995).

- ¹⁹L. D. Landau and E. M. Lifschitz, *Statistical Physics* (Pergamon, New York, 1959), p. 365.
- ²⁰Z. Adamczyk, B. Siwek, M. Zembala, and P. Weroński, *J. Colloid Interface Sci.* (in press).
- ²¹J. G. Goodwin, J. Hearn, C. C. Ho, and R. H. Ottewill, *Colloid Polym. Sci.* **252**, 464 (1974).
- ²²Z. Adamczyk, M. Zembala, B. Siwek, and P. Warszyński, *J. Colloid Interface Sci.* **140**, 123 (1990).
- ²³Z. Adamczyk and P. Warszyński, *Adv. Colloid Interface Sci.* **63**, 41 (1996).
- ²⁴J. Sjollem and H. J. Busscher, *Colloids Surf.* **47**, 337 (1990).
- ²⁵Z. Adamczyk, B. Siwek, and M. Zembala, *Colloids Surf.* **62**, 119 (1992).
- ²⁶Z. Adamczyk and P. Weroński, *Langmuir* **11**, 4400 (1995).
- ²⁷D. Henderson and S. G. Davison, in *Physical Chemistry, An Advanced Treatise* (Academic Press, New York, 1967), Vol. II, Chap. 7, pp. 364, 382.